Regular Article

LYMPHOID NEOPLASIA

Humanized *Mcl-1* mice enable accurate preclinical evaluation of MCL-1 inhibitors destined for clinical use

Margs S. Brennan,[1,2] Catherine Chang,[1] Lin Tai,[1] Guillaume Lessene,[1-3] Andreas Strasser,[1,2] Grant Dewson,[1,2] Gemma L. Kelly,[1,2,*] and Marco J. Herold[1,2,*]

[1]The Walter and Eliza Hall Institute of Medical Research, Melbourne, Australia; and [2]Department of Medical Biology and [3]Department of Pharmacology and Therapeutics, University of Melbourne, Melbourne, Australia

KEY POINTS

- Due to the higher affinity of current MCL-1 inhibitors, *huMcl-1* mice have been established.

- A therapeutic window for S63845 can be established in *huMcl-1* mice transplanted with *huMcl-1;Eμ-Myc* lymphomas.

Myeloid cell leukemia-1 (MCL-1) is a prosurvival B-cell lymphoma 2 (BCL-2) family member required for the sustained growth of many cancers. Recently, a highly specific MCL-1 inhibitor, S63845, showing sixfold higher affinity to human compared with mouse MCL-1, has been described. To accurately test efficacy and tolerability of this BH3-mimetic (BH3-only protein mimetic) drug in preclinical cancer models, we developed a humanized *Mcl-1* (*huMcl-1*) mouse strain in which MCL-1 was replaced with its human homolog. *huMcl-1* mice are phenotypically indistinguishable from wild-type mice but are more sensitive to the MCL-1 inhibitor S63845. Importantly, nontransformed cells and lymphomas from *huMcl-1; Eμ-Myc* mice are more sensitive to S63845 in vitro than their control counterparts. When *huMcl-1;Eμ-Myc* lymphoma cells were transplanted into *huMcl-1* mice, treatment with S63845 alone or alongside cyclophosphamide led to long-term remission in ~60% or almost 100% of mice, respectively. These results demonstrate the potential of our *huMcl-1* mouse model for testing MCL-1 inhibitors, allowing precise predictions of efficacy and tolerability for clinical translation. (*Blood*. 2018;132(15):1573-1583)

Introduction

Apoptosis is a form of programmed cell death that removes unwanted and potentially dangerous cells in multicellular organisms.[1] Deregulation of apoptosis can result in accumulation of cells that should normally be deleted. The abnormal proliferation of mutated "undead" cells can lead to tumor development.[2] Cell death hinges on the balance between the prosurvival and proapoptotic members of the B-cell lymphoma 2 (BCL-2) family of proteins. This family is divided into the prosurvival members (BCL-2, BCL–extra large [BCL-X$_L$], BCL-WEHI [BCL-W], myeloid cell leukemia-1 [MCL-1], and BCL-2–related protein A1 [BCL2A1]/BFL-1), the BCL-2 homology domain 3 (BH3)-only proapoptotic proteins (eg, BCL-2 interacting mediator of cell death [BIM] and p53-upregulated modulator of apoptosis [PUMA]), and the multi-BH domain proapoptotic effectors (BCL-2 homologous antagonist/killer [BAK], BCL-2–associated X protein [BAX], and BCL-2–related ovarian killer [BOK]).[3] Diverse stress stimuli induce expression of BH3-only proteins to initiate apoptosis, either indirectly by binding to the prosurvival BCL-2 proteins, thereby unleashing the proapoptotic effectors BAK and BAX, or by binding BAK and BAX directly. Following activation, BAK and BAX oligomerize on the outer mitochondrial membrane, perforating its surface, releasing cytochrome c and other apoptogenic factors. This unleashes the caspase cascade that causes demolition of the cell.[3,4]

Cancer cells can subvert the apoptotic machinery by upregulation of prosurvival, or downregulation of proapoptotic proteins.[2] The *MCL-1* locus is amplified in numerous human tumor types,[5] and functional studies in mouse models showed that MCL-1 is essential for the sustained growth of hematopoietic[6-11] cancers,[6-11] and some solid tumor subtypes.[12,13] Direct targeting of prosurvival BCL-2 family members with BH3 mimetics has proven success as cancer therapy. The BCL-2 inhibitor venetoclax is highly efficacious for the treatment of relapsed/refractory chronic lymphocytic leukemia (CLL).[14,15] A clinically relevant specific and potent MCL-1 inhibitor, S63845,[16] was shown to be efficacious as a monotherapy in several preclinical models of hematological malignancies and in combination with oncogenic kinase inhibitors in certain lung-, skin-, and breast cancer–derived cell lines and patient-derived xenograft models.[16-18]

The clinical application of MCL-1 inhibitors has been of substantial concern given the important prosurvival role of MCL-1 in many normal tissues. MCL-1 is widely expressed,[19] and essential for embryonic development with homozygous *Mcl-1* loss in mice resulting in failure to implant at the blastocyst stage.[20] Conditional gene knockout studies showed that MCL-1 plays a vital role in the survival of cardiomyocytes,[21,22] hematopoietic stem cells,[23] developing and mature lymphocytes,[24-28] and in the maintenance of oocytes in the ovarian reserve.[29] Despite these reports, little toxicity was observed in mice treated with doses
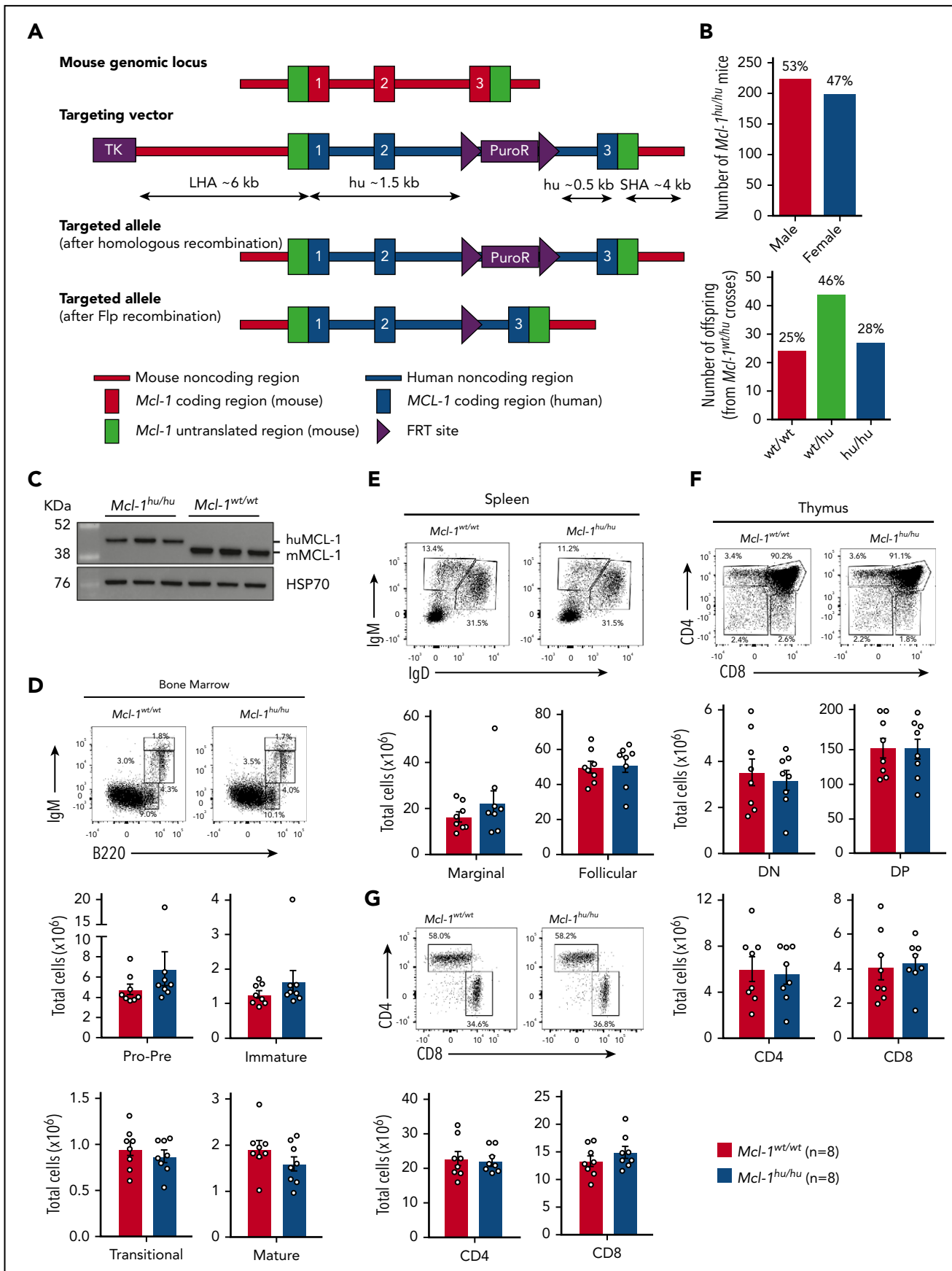
Figure 1.

of the MCL-1 inhibitor S63845 that ablates mouse lymphoma cells.[16] One caveat of these results is that S63845 has an approximately sixfold higher affinity for the human compared with the mouse MCL-1 protein and it is therefore possible that the mouse models used were not sensitive enough to reveal potential on-target toxicities. Thus, it was pivotal to more accurately test the MCL-1 inhibitor S63845 in a preclinical model in which the *Mcl-1* locus was humanized (*huMcl-1*) by replacing the native coding region of the murine *Mcl-1* locus with the *huMCL-1* coding sequence. These *huMcl-1* mice are healthy and fertile, and the intrinsic apoptotic pathway is intact in their cells, demonstrating that the huMCL-1 protein can functionally fully replace the murine protein. As predicted, cells from *huMcl-1* mice were more sensitive to the MCL-1 inhibitor S63845 compared with wild-type mouse cells, but not to other cytotoxic agents that induce apoptosis. Accordingly, the maximum tolerated dose of S63845 was lower in the *huMcl-1* mice compared with their wild-type counterparts. However, it was still possible to determine a therapeutic window for S63845 treatment, both alone and in combination with cyclophosphamide (CP), in a MYC-driven lymphoma model expressing huMCL-1. These findings demonstrate the utility of the *huMcl-1* model to accurately determine the efficacy and tolerability of S63845 and potentially other MCL-1 inhibitory drugs in preclinical models of disease.

Materials and methods

Generation of huMcl-1 mice

Mice bearing the *huMcl-1* allele were generated by Taconic Biosciences GmbH (Cologne, Germany). The targeting vector (Figure 1A) was transfected into the TaconicArtemis C57BL/6NTac embryonic stem (ES) cell line. Correctly targeted ES cells were injected into BALB/c blastocysts that were transferred into pseudopregnant NMRI females to generate chimeric offspring for further breeding. The flippase recognition target (FRT) site–flanked *PuroR* selection cassette was removed by crossing chimeric mice with the flippase (Flpe)-expressing C57BL/6-Tg (CAG-Flpe)2 Arte mice. Genotyping was performed by polymerase chain reaction (PCR) to confirm cassette removal, loss of the Flpe transgene, and presence of the wild-type or humanized *Mcl-1* alleles (for PCR primers used, see supplemental Table 1, available on the *Blood* Web site).

Coimmunoprecipitation, subcellular fractionation, and western blotting

Thymocytes were isolated from *Mcl-1^wt/wt^* and *Mcl-1^hu/hu^* mice; coimmunoprecipitation and subcellular fractionation was performed as described previously.[30] For immunoprecipitation, 2.5 µg of monoclonal antibody (14C11-20) against MCL-1[31] and G sepharose beads were used before being analyzed

by western blotting (antibodies listed in supplemental Table 2). For all other western blots, cell lysates were prepared in radioimmunoprecipitation assay (RIPA) buffer (supplemental Table 3) supplemented with cOmplete protease inhibitor (Roche). Protein concentration was determined by Bradford assay using the Protein Assay Dye Reagent Concentrate (Bio-Rad, Hercules, CA). Samples of 15 µg of protein were prepared in Laemmli buffer (supplemental Table 3), boiled for 5 minutes, and size-fractionated by gel electrophoresis on NuPAGE 10% Bis-Tris 1.5-mm gels (Life Technologies) in 2-(N-morpholino)ethanesulfonic acid (MES) buffer and then transferred onto nitrocellulose membranes (Life Technologies) using the iBlot membrane transfer system. Antibody dilution and blocking were performed in 5% skim milk, 0.1% Tween 20 in phosphate-buffered saline (PBS). For antibodies, refer to supplemental Table 3, in-house antibodies.[31,32] Luminata Forte Western horseradish peroxidase (HRP) substrate (Millipore, Billerica, MA) was used for developing the signal, and membranes were imaged and analyzed using the ChemiDoc XRS+ machine with ImageLab software (Bio-Rad).

Immunostaining and flow cytometry

Thymus, spleen, and bone marrow were harvested and single-cell suspensions prepared in PBS (Gibco), 5 mM EDTA (Merck), supplemented with 5% fetal bovine serum (FBS; Sigma-Aldrich) for staining. Monoclonal antibodies (supplemental Table 4) were obtained from eBioscience, BioLegend, or generated in-house. Streptavidin-phycoerythrin (PE; BioLegend) was used to detect biotinylated antibodies. Propidium iodide (PI; 1 µg/mL) was used to exclude dead cells. Whole-organ cell counts were determined by the CASY counter (Schärfe System GmbH) (Figure 1; supplemental Figure 1) or by mixing a known concentration of APC Calibrite beads (Becton Dickinson) with each sample (Figure 3; supplemental Figure 3). Data were collected using LSR II, LSRFortessa, or LSRFortessa X-20 analyzers and examined using FlowJo 10 (Becton Dickson).

Tissue-culture and cell-viability assays

Eµ-Myc lymphoma cell lines were maintained as previously described.[9] For all experiments, viability was determined by resuspending cells in Annexin V–binding buffer (0.1 M N-2-hydroxyethylpiperazine-N′-2-ethanesulfonic acid [HEPES; pH 7.4], 1.4 M NaCl, 25 mM CaCl$_2$) containing PI (1 µg/mL) and fluorescein isothiocyanate (FITC)- or Alexa Fluor 647–conjugated Annexin V (generated in-house). Spleen and thymi were harvested and single-cell suspensions prepared. To isolate B cells, splenocytes were pelleted and resuspended in 1 mL of red cell lysis buffer (156 mM ammonium chloride [BDH], 11.9 mM sodium bicarbonate [Merck], EDTA [Sigma-Aldrich]) for 5 minutes to deplete erythrocytes. Cells were then stained with biotinylated antibodies against CD4, CD8, MAC-1, and

Figure 1. Humanized *Mcl-1* mice show no defects under steady-state conditions. (A) Schematic representation of the murine *Mcl-1* gene locus, the *huMcl-1* targeting vector and the correctly targeted alleles, before and after Flpe-mediated recombination. (B) Offspring sex frequency of *Mcl-1^hu/hu^* mice and Mendelian ratios from intercrosses of *Mcl-1^wt/wt^* mice. (C) Thymocytes were isolated from *Mcl-1^hu/hu^* and *Mcl-1^wt/wt^* mice. MCL-1 protein (mouse and human) expression was detected by western blotting. Probing for heat shock protein 70 (HSP70) served as a loading control. (D-G) Single-cell suspensions were prepared from spleen, thymus and bone marrow of *Mcl-1^hu/hu^* and *Mcl-1^wt/wt^* mice and cell subsets were determined by immunostaining and FACS analysis. Data are presented as mean ± SEM, significance determined by the Student *t* test. (D) Representative FACS plot of B-cell development in the bone marrow (top) and total cell numbers per femur (bottom panels). Pro-B/pre-B (B220^lo^IgM⁻), immature B (B220^lo^IgM^mid^), transitional B (B220^lo-hi^IgM^hi^), and mature (B220^hi^IgM^mid^) B cells. (E) Representative FACS plot of peripheral B cells in the spleen (top) and total cell number (bottom). B cells defined as follicular (IgM⁺IgD⁺) and marginal zone (IgM⁺IgD^lo^) B cells. (F) Representative FACS plot analyzing T-cell development in the thymus (top) and total cell numbers calculated for each population (bottom panels). Immature double-negative thymocytes (DN; CD4⁻CD8⁻), double-positive thymocytes (DP; CD4⁺CD8⁺), and the mature CD4 and CD8 single-positive populations. (G) Representative FACS plot of peripheral T cell distribution (top) in the spleen as well as total cell numbers of CD4 and CD8 single-positive T cell populations (bottom panel). Ig, immunoglobulin.
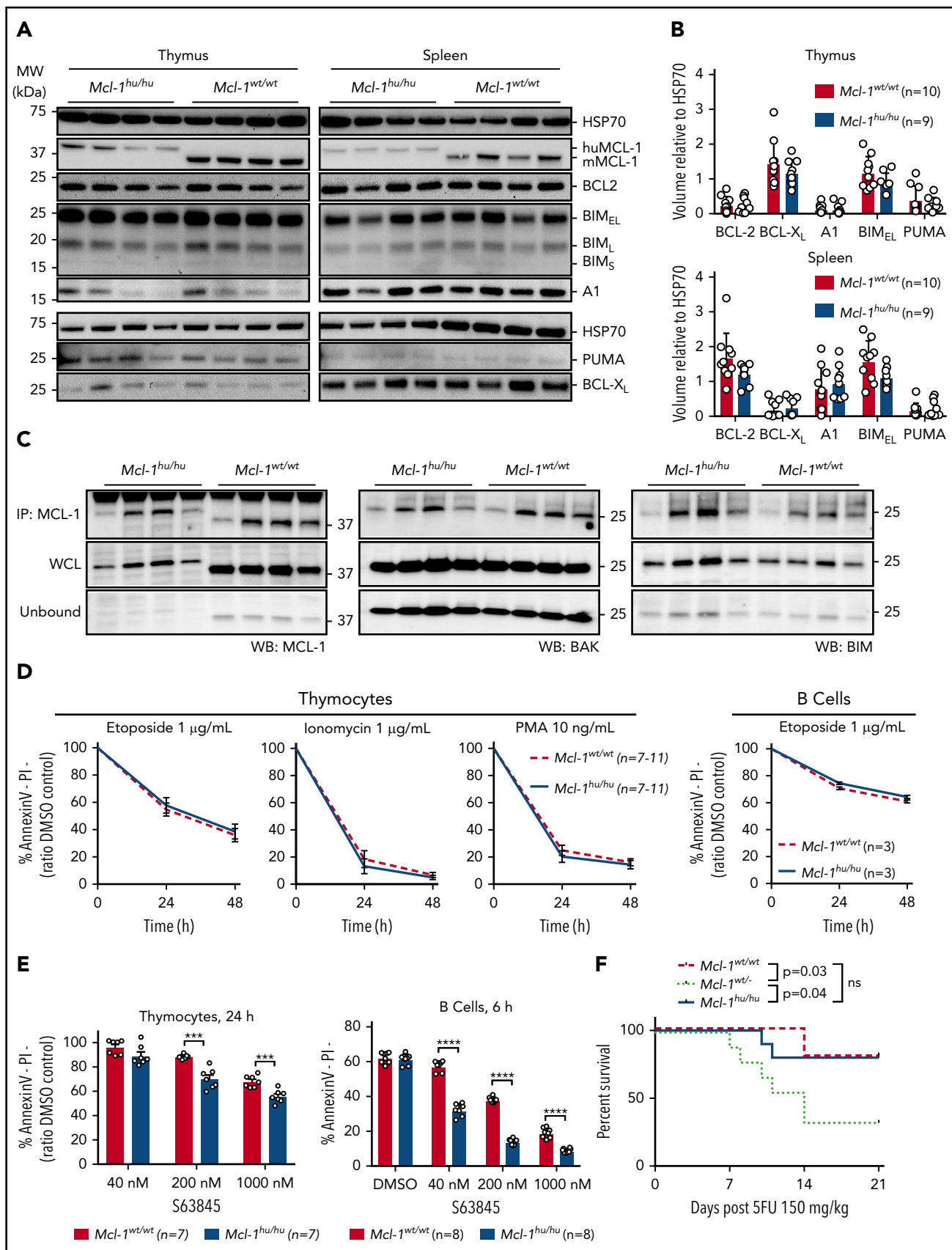
Figure 2. The apoptosis machinery remains intact in humanized *Mcl-1* mice. (A) Thymocytes and splenocytes were isolated from *Mcl-1$^{hu/hu}$* and *Mcl-1$^{wt/wt}$* mice. Expression of MCL-1, BCL-2, BCL-X$_L$, A1, BIM, and PUMA was detected by western blotting. Probing for HSP70 served as a loading control. Representative blots are shown. (B) Quantification of expression levels of BCL-2 family proteins in thymocytes and splenocytes from *huMcl-1* (n = 9) and wild-type (n = 10) mice determined by western blotting. Chemiluminescent

BRENNAN et al

GR-1 (supplemental Table 4) to enrich for B cells by MagniSort Streptavidin Negative Selection Beads (Thermo Fisher), as per the manufacturer's protocol. Isolated B cells and thymocytes, and Eμ-Myc lymphoma cell lines, were seeded at 5×10^4 cells per well in media,[9] in triplicate per condition, in 96-well flat-bottomed plates and treated with indicated drugs (S63845 [Servier], dexamethasone, etoposide, phorbol myristate acetate [PMA], ionomycin [Sigma-Aldrich], ABT-199 [Active Biochem]) for the indicated times. The 50% inhibitory concentration (IC_{50}) values were determined using nonlinear regression algorithms in Prism (GraphPad).

Animals and in vivo drug treatments

The care and use of mice for experimental purposes were carried out in accordance with the requirements set out by The Walter and Eliza Hall Institute (WEHI) Animal Ethics Committee. HuMcl-1 mice are described in "Generation of huMcl-1 mice"; Eμ-Myc[33] and Mcl-1[+/−][25] have been described previously. All mice are kept on a C57BL/6-Ly5.2 background. The huMcl-1 allele was bred onto a C57BL/6-Ly5.1 background for use as recipient animals for all transplant experiments. Single-cell suspensions of 1×10^5 Eμ-Myc lymphoma (Ly5.2) cells in PBS were injected into 8- to 12-week-old huMCL-1;Ly5.1 recipient mice by IV tail-vein injection. Recipient mice were sex matched to transplanted tumors. Working solutions of cyclophosphamide (CP) and 5-fluorouracil (5-FU; Sigma-Aldrich) were prepared in PBS. CP was administered by intraperitoneal injection, 5-FU by IV tail-vein injection. S63845 (Servier) was formulated extemporaneously and protected from light in 2% vitamin E/d-α-tocopheryl polyethylene glycol 1000 succinate (Sigma-Aldrich) in NaCl 0.9% (wt/vol) and delivered by IV tail-vein injection at the indicated doses and schedule. Mice were monitored for sickness and euthanized when deemed unwell by experienced mouse technicians.

Statistical analysis

Prism software (GraphPad) was used to generate survival curves and perform all statistical testing of data. All data are presented as mean plus or minus standard error of the mean (SEM) unless stated otherwise. P values of $<.05$ were considered significant.

Results

Generation of the huMcl-1 mouse model

The humanized Mcl-1 (huMcl-1) mouse model was generated by standard gene targeting in C57BL/6 ES cells. Expression of the huMCL-1 protein under the control of the murine Mcl-1 regulatory regions was achieved by substitution of the exons and interspersing introns of the mouse Mcl-1 locus with the huMCL-1 exon/intron sequences, while maintaining the flanking 5' and 3' untranslated regions (UTR) of the genomic locus of the mouse (Figure 1A). Homozygous loss of Mcl-1 causes embryonic lethality

prior to embryonic day 4 in mice.[20] Furthermore, changes in the 5' UTR of the murine Mcl-1 locus resulted in infertility in homozygous male Mcl-1 floxed mice.[31,34] Importantly, the humanization of MCL-1 in mice had no impact on embryonic development or fertility in both female and male Mcl-1[hu/hu] offspring, with the expected Mendelian ratios and sex distribution observed in intercrosses of Mcl-1[wt/hu] mice (Figure 1B). Western blot analysis of thymocytes from huMcl-1 mice showed efficient expression of the huMCL-1 protein, as evidenced by the predicted size difference between the mouse and huMCL-1 proteins (human, 38 kDa; mouse, 35 kDa; Figure 1C). A cohort of huMcl-1 mice was aged for >600 days with no obvious defects evident.

### huMcl-1 mice have normal hematopoietic cell subset distribution

Fluorescence-activated cell sorter (FACS) analysis of the bone marrow revealed no differences in the frequencies and numbers of pro-B/pre-B (B220[lo]IgM[−]), immature B (B220[lo]IgM[+]), transitional B (B220[mid]IgM[hi]), or mature B (B220[hi]IgM[lo]) cell subsets between huMcl-1 mice and wild-type controls (Figure 1D). There were also no abnormalities in IgM[+] or IgD[+] peripheral B lymphocytes in the huMcl-1 mice (Figure 1E). The frequencies and numbers of the stages of thymocyte development, as determined by staining for CD4 and CD8, were also comparable between huMcl-1 mice and wild-type controls (Figure 1F). Moreover, huMcl-1 mice had normal frequencies and numbers of mature CD4^{+} and CD8^{+} T lymphocytes in the spleen (Figure 1G), with normal distributions of naive (CD62L^{+}CD44^{−}), effector memory (CD62L^{−}CD44^{+}), and central memory (CD62L^{+}CD44^{+}) CD4^{+} T cells (supplemental Figure 1A). Finally, the huMcl-1 mice had no perturbations in macrophage/monocyte (MAC-1^{+}GR-1^{lo}) and neutrophil populations (MAC-1^{+} GR-1^{hi}) in the bone marrow and spleen (supplemental Figure 1B).

huMCL-1 protein can functionally replace mouse MCL-1 within the apoptotic machinery

It is possible that other BCL-2 family proteins are differentially expressed to compensate for the expression of huMCL-1 instead of mouse MCL-1 protein in vivo. To investigate this, we carried out western blotting on protein extracted from thymocytes and splenocytes from huMcl-1 mice and wild-type controls. No differences in expression of proapoptotic BIM and PUMA or prosurvival BCL-2, BCL-XL, or A1 were observed (Figure 2A-B). The affinities of the antibodies used to detect the mouse MCL-1 vs huMCL-1 proteins is unknown, thus we could not compare the relative protein expression by western blot. To assess whether the huMCL-1 protein expressed in mouse cells can interact with the endogenous mouse proapoptotic BCL-2 relatives, co-immunoprecipitation assays were performed on thymocyte extracts. This revealed that in mouse cells, the huMCL-1 protein could bind mouse BIM and BAK in a similar manner as mouse MCL-1 (Figure 2C). Additionally, subcellular fractionation of

Figure 2 (continued) signals from each protein were normalized to the HSP70 loading control signal and plotted as arbitrary units; significance calculated by multiple Student t tests. (C) Lysates were prepared from thymocytes from huMcl-1 and wild-type mice and subjected to immunoprecipitation with an MCL-1 (binds both the mouse MCL-1 and huMCL-1 proteins) specific antibody. The immunoprecipitated material was immunoblotted for MCL-1 (left panel), BAK (middle panel), and BIM (right panel). Pulled-down fraction shown in top panels with whole-cell lysate (WCL) and unbound fractions shown below. (D) Thymocytes and splenic B cells were isolated from huMcl-1 and wild-type mice and exposed in culture to the indicated cytotoxic stimuli. Cell viability at 24 and 48 hours was assessed by Annexin V/PI staining and FACS analysis. (E) Thymocytes and splenic B cells were isolated from huMcl-1 and wild-type mice and treated with the MCL-1 inhibitor S63845 at the indicted concentrations. Cell viability at indicated time points was assessed by Annexin V/PI staining and FACS analysis. Data are presented as mean ± SEM; significance calculated by multiple Student t tests at each time point; *P < .05, **P < .01, ***P < .001, ***P < .0001. (F) Mice of the indicated genotypes were treated with a single dose of 150 mg/kg body weight 5-FU and survival monitored. Kaplan-Meier curves are shown; statistical analysis was performed by the log-rank (Mantel-Cox) test; *P < .05. DMSO, dimethyl sulfoxide; IP, immunoprecipitation; MW, molecular weight; ns, not significant; WB, western blot.
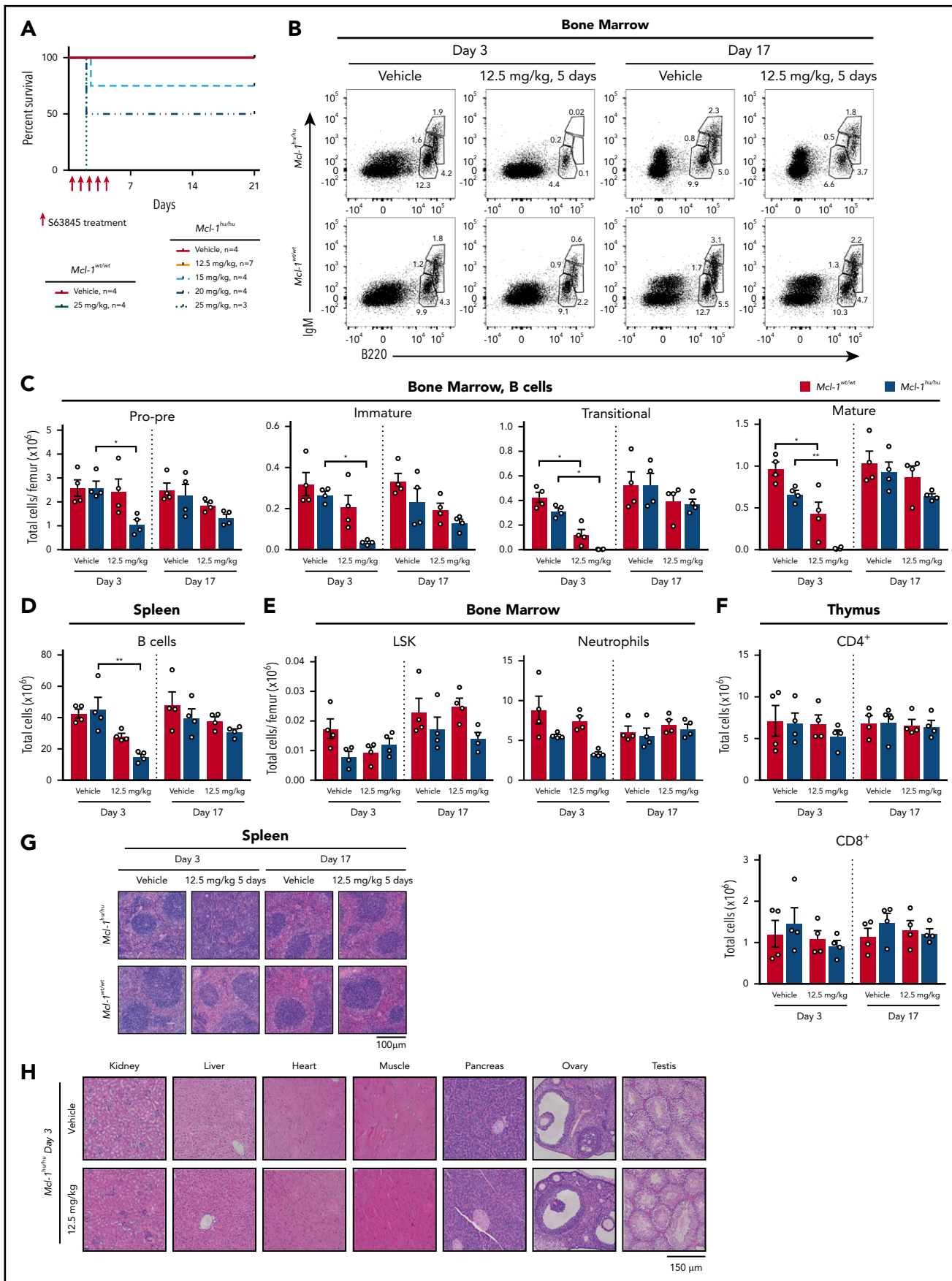
Figure 3.

thymocytes and splenocytes showed that huMCL-1 is mainly localized to the mitochondrial outer membrane, as is the case for mouse MCL-1 (supplemental Figure 2A). It is reported that the MCL-1 protein is stabilized upon binding to S63845.[16] Stabilization of both huMCL-1 and mouse MCL-1 protein was evident in thymocytes isolated from $Mcl-1^{wt/hu}$ heterozygous mice that were treated ex vivo with S63845 (supplemental Figure 2B). To functionally assess the huMCL-1 protein, cells from the $huMcl-1$ mice and wild-type control mice were exposed to different cytotoxic stimuli in vitro. Importantly, survival of thymocytes and B cells from the $huMcl-1$ mice and control mice were comparable (Figure 2D). As predicted, thymocytes and B cells from the $huMcl-1$ mice were more sensitive to the MCL-1 inhibitor S63845 than those from wild-type mice (Figure 2E). The increased sensitivity to S63845 only became obvious at higher doses in thymocytes. This is likely due to the fact that $CD4^+CD8^+$ thymocytes rely on both MCL-1 and BCL-X_L for survival.[27] More striking differences were observed in B cells after 6 hours of treatment at lower doses of the MCL-1 inhibitor (Figure 2E; supplemental Figure 2C). In determining the IC_{50} of S63845, it became apparent that the huMCL-1–expressing B cells are about 7 or 4 times more sensitive to this compound compared with their wild-type counterparts at 24 h and 48 h, respectively (supplemental Figure 2D-E).

Next, the ability of huMCL-1 protein expressed in mouse cells to function within a whole animal was examined. MCL-1 is required for the maintenance of hematopoietic stem/progenitor cells[23] and also for emergency hematopoiesis following myeloablative chemotherapy.[35] The latter was demonstrated by the observation that $Mcl-1^{wt/-}$ mice were compromised in their recovery following 5-FU treatment. We exposed $huMcl-1$, $Mcl-1^{wt/-}$ (as a control), and wild-type mice to a single dose of 5-FU (150 mg/kg body weight) and examined hematopoietic recovery over a 21-day period. As reported,[35] most $Mcl-1^{wt/-}$ mice did not recover from 5-FU treatment, whereas $huMcl-1$ mice recovered as well as the wild-type controls (Figure 2F). Collectively, these findings demonstrate that huMCL-1 is functional and the overall apoptotic machinery is intact in cells from the $huMcl-1$ mice, both in vitro and in vivo. Furthermore, as predicted, these cells show increased sensitivity to the MCL-1 inhibitor S63845.

Determining the maximum tolerated dose of S63845 in huMcl-1 mice

Given the binding affinity of S63845 is approximately sixfold higher for huMCL-1 compared with mouse MCL-1 protein,[16] we determined the maximum tolerated dose (MTD) of S63845 in the $huMcl-1$ mice. Treatment of $huMcl-1$ mice on 5 consecutive days IV with doses ranging from 5 to 25 mg/kg body weight established an MTD of S63845 as high as 12.5 mg/kg (Figure 3A). All mice treated with 25 mg/kg S63845 needed to be euthanized

due to increased respiration and inability to rise or ambulate. However, the exact cause of death could not be determined. Because the tolerability of the drug was considerably higher in wild-type mice, which all survived the 25 mg/kg dosing schedule (Figure 3A) and have previously been shown to have an MTD of 40 mg/kg,[16] this demonstrates that the $huMcl-1$ mice are more sensitive to the MCL-1 inhibitor S63845.

S63845 exerts no enduring toxicity in the huMcl-1 mice at the MTD

There have been many reports on the importance of MCL-1 in several vital tissues[21-29] raising the question of whether an MCL-1 inhibitor would find its therapeutic use in the clinic. Previously and unexpectedly, it was shown that S63845 exerts very little toxic effects at the MTD in mice expressing mouse MCL-1.[16] However, given the higher affinity of S63845 for huMCL-1, we revisited this finding by treating $huMcl-1$ and wild-type control mice for 5 consecutive days with either vehicle or 12.5 mg/kg S63845 and monitored the acute impact and recovery 3 or 17 days posttreatment, respectively. In the $huMcl-1$ mice, the pro-B/pre-B (B220^{lo}IgM$^-$), immature B (B220^{lo}IgM$^+$), transitional B (B220^{mid}IgM^{hi}), and mature B (B220^{hi}IgM^{lo}) B cells in the bone marrow were significantly reduced at 3 days but mostly recovered at 17 days posttreatment (Figure 3B-C). Similar observations were made for B cells in the blood (supplemental Figure 3A) and spleen (Figure 3D). Despite the reduction in splenic B cells, an increase in cellularity was noted in the spleens of all $huMcl-1$ mice treated with S63845 3 days following treatment, but these values normalized at 17 days posttreatment (supplemental Figure 3B). FACS analysis revealed that the increased splenic cellularity was due to an increase in EryA (Lineage$^-$Ter119^{hi}CD71$^+$ FSC-A^{hi}) and EryB (Lineage$^-$Ter119^{hi}CD71$^+$FSC-A^{lo}) erythrocyte progenitor populations, with the more mature EryC (Lineage$^-$Ter119^{hi}CD71$^-$FSC-A^{lo}) remaining stable throughout the experiment (supplemental Figure 3D). Moreover, the red blood cell counts in the blood showed a modest reduction at day 3 posttreatment, but again these numbers completely recovered at day 17 (supplemental Figure 3E). No significant changes were observed in the Lineage$^-$SCA-1$^+$c-KIT$^+$ (LSK) population in the bone marrow (Figure 3E) of the S63845-treated $huMcl-1$ mice. A trend toward neutrophil reduction in the bone marrow was seen at day 3, however, this did not reach statistical significance (Figure 3E). No reductions in neutrophils were seen in the spleen (supplemental Figure 3F). Moreover, there were no changes in the numbers of mature CD4$^+$ and CD8$^+$ T cells (Figure 3F), immature double-negative (DN1-4; Lineage$^-$TCRb$^-$CD4$^-$CD8$^-$), and double-positive (DP; CD4$^+$CD8$^+$) thymocytes or mature T cells (T-cell receptor β–positive) in the spleen of S63845-treated $huMcl-1$ mice (supplemental Figure 3G). Histological analysis revealed increased size and loss

Figure 3. S63845 exerts no enduring toxicity in the *huMcl-1* mouse model at the MTD. (A) Kaplan-Meier survival curves of *huMcl-1* or wild-type mice treated for 5 consecutive days with vehicle or increasing doses of S63845, as indicated. (B-H) The *huMcl-1* and wild-type mice were treated with 5 consecutive doses of 12.5 mg/kg S63845 or vehicle. At 3 or 17 days posttreatment, organs were harvested for analysis. (B-F) Single-cell suspensions were prepared from spleen, thymus, and bone marrow of *Mcl-1*$^{hu/hu}$ and *Mcl-1*$^{wt/wt}$ mice and cell subsets were determined by immunostaining and FACS analysis. Data are presented as mean ± SEM, significance determined by the Student *t* test. *P < .05, **P < .01. (B) Representative FACS plot of B cells in the bone marrow and (C) total cell numbers per femur. B cells defined as pro-B/pre-B (B220^{lo}IgM$^-$), immature B (B220^{lo}IgM^{mid}), transitional B (B220^{lo-hi}IgM^{hi}), and mature B cells (B220^{hi}IgM^{lo}). (D) Total numbers of B cells in the spleen (B220$^+$) (E) LSK cells (Lineage$^-$SCA-1$^+$c-KIT$^+$) and macrophages/monocytes (MAC-1$^+$GR-1^{lo}) in the bone marrow (F) and mature T cells (CD4$^+$ or CD8$^+$) in the thymus at indicated time points. (G) Representative hematoxylin-and-eosin (H&E)-stained section of spleens from *huMcl-1* or wild-type mice that had been treated with 12.5 mg/kg S63845 or vehicle and were harvested at either 3 or 17 days posttreatment. (H) Representative H&E-stained sections of various organs, as indicated, from *huMcl-1* mice treated with 5 consecutive doses of 12.5 mg/kg S63845 or vehicle 3 days after treatment had ceased.

of normal architecture of the spleen, which complements the FACS data (Figure 3G). Histological analysis of major organs revealed no damage in response to S63845 (Figure 3H). These data indicate that S63845 treatment can be tolerated in *huMcl-1* mice, with only a transient reduction of certain hematopoietic cell subsets.

Eμ-Myc cell lines expressing huMCL-1 are more sensitive to S63845

To test whether malignant cells also demonstrated an increased sensitivity toward MCL-1 inhibition with S63845, *huMcl-1* mice were crossed with the *Eμ-Myc*–transgenic animals. Although the latency and tumor phenotype did not differ between mouse or huMCL-1–expressing *Eμ-Myc* mice (Figure 4A-B), the in vitro sensitivity of lymphoma cell lines generated from sick *Eμ-Myc;huMcl-1* mice toward S63845 was approximately sixfold higher compared with control *Eμ-Myc* lymphoma cells expressing mouse MCL-1 (25 nM vs 160 nM, respectively; Figure 4C-D). Conversely, there was no significant difference in sensitivity when these cells were treated with etoposide or the BCL-2–specific BH3 mimetic ABT-199/venetoclax (supplemental Figure 4A-B), providing evidence that the increased sensitivity is due to the higher affinity of S63845 to the huMCL-1 protein.

Regression of huMcl-1;Eμ-Myc lymphomas in vivo after treatment with S36845, either alone or in combination with cyclophosphamide

To test the sensitivity of *Eμ-Myc* lymphomas expressing huMCL-1 to S63845 in vivo, we transplanted *huMcl-1;Eμ-Myc* lymphoma cell lines into *huMcl-1;Ly5.1* recipient mice (ie, both lymphoma and normal cells expressed huMCL-1). After 3 days, mice were treated for 5 consecutive days with vehicle or 12.5 mg/kg S63845 and monitored for signs of sickness. Sixty percent of mice were cured at this dose (Figure 4E; supplemental Figure 4C). Next, we aimed to improve tumor-free survival in mice transplanted with *huMcl-1;Eμ-Myc* lymphoma cell lines. To this end, *huMcl-1;Eμ-Myc* lymphoma cell lines were transplanted into *huMcl-1;Ly5.1* recipient mice and 2 days later treated with vehicle or a low dose of CP (50 mg/kg). Three days later, mice were treated for 5 consecutive days with a low dose of S63845 (7.5 mg/kg). Treatment with 50 mg/kg CP or 7.5 mg/kg S63845 by themselves resulted in ~50% or ~25% long-term tumor-free survival, respectively. Excitingly though, only 1 mouse became sick with lymphoma in the CP plus S63845 combination treatment, thereby increasing the tumor-free survival to almost 100% (Figure 4F; supplemental Figure 4D). For *Eμ-Myc* lymphoma lines that previously showed regression at 12.5 mg/kg body weight S63845 (hME160, hME184, hME273; supplemental Figure 4C), tumor-free survival could be achieved with as little as 3.75 mg/kg body weight S63845 in combination with CP (Figure 4G). These findings, in a highly relevant mouse model in which both the lymphoma cells and the normal cells express huMCL-1, clearly demonstrate that there is a therapeutic window for S63845, and that the efficacy can be enhanced by combining treatment with cyclophosphamide.

Discussion

Here, we describe a novel humanized *Mcl-1* mouse model, in which huMCL-1 protein is expressed instead of mouse MCL-1 under the control of the mouse *Mcl-1* regulatory regions. Normal embryonic development and fertility of the *Mcl-1*[hu/hu] mice is noteworthy given that even small changes to the *Mcl-1* locus

or loss of only 1 allele have consequences in adult mice,[31,34] with homozygous loss of *Mcl-1* being very early embryonic lethal.[20] Notably, the intrinsic apoptotic pathway remains intact in cells from the *huMcl-1* mice with no detectable compensatory changes in the levels of other antiapoptotic or proapoptotic BCL-2 family proteins (Figure 2). This is critical because the expression of certain BCL-2 family member(s) could be expected to change to compensate for loss of another. For example, tumor cells can acquire resistance to inhibitors of BCL-2, BCL-XL, and BCL-W (eg, ABT-737) by upregulating MCL-1.[36] Because the *huMcl-1* mice are normal and their cells have normally functioning apoptotic machinery, they represent an ideal model to predict tolerability and efficacy of MCL-1 inhibitors.

MCL-1 is regarded as an exciting therapeutic target due to its requirement for the sustained growth of many cancers, and S63845 has been developed as a highly selective and potent MCL-1 inhibitor. A so-far unique feature for BH3 mimetics is that S63845 binds more tightly to human compared with mouse MCL-1, and one could imagine that any newly generated compounds targeting MCL-1 would likely bind in the same region, and therefore, will likely have similar properties. Because previous in vivo experiments have all been conducted with mouse MCL-1 as the target, it was difficult to ascertain whether the results are truly reflective of the therapeutic potential of S63845 and, perhaps more importantly, its safety. Our studies using the *huMcl-1* mouse model support the notion that a therapeutic window for MCL-1 inhibitors might be established, with a transient loss of B cells being the most significant side effect observed at doses of S63845 that could halt lymphoma growth in a substantial fraction of mice. These data may be viewed as conflicting with previous data showing the importance of MCL-1 in many essential normal cell types, such as cardiomyocytes. We believe that the lack of significant side effects is due to the transient action and hence inhibition of MCL-1 by S63845, in contrast to the irreversible loss of MCL-1 elicited by genetic deletion. Additionally, it is not yet known whether administered S63845 is available in all organs throughout the mouse, which may further explain the differences seen between genetic deletion vs drug-mediated inhibition of MCL-1. Further pharmacokinetic studies must be performed to address this question.

Although S63845 appears to be relatively well tolerated, as previously shown in mice expressing mouse MCL-1, we have shown that S63845's higher affinity for huMCL-1 vs mouse MCL-1 is relevant in vivo with the MTD of S63845 in *huMcl-1* mice being ~3 times lower than that seen in wild-type mice. Although the MTD of S63845 was determined within a 5-day treatment window only, it would also be desirable to determine the MTD after a much longer treatment period to mimic potential clinical use as applied for other inhibitors of prosurvival BCL-2 proteins, such as ABT-199/venetoclax.[14] However, we are unable to carry out these experiments due to animal ethics restrictions that regulate the number of daily IV injections that a mouse can receive, particularly if a curative regime can be achieved with fewer injections as demonstrated in this study (Figure 4). We anticipate that the the *huMcl-1* mouse model will be invaluable for future preclinical work using S63845 (and other MCL-1 inhibitors) for determining a therapeutic window for treatment of cancers and possibly other diseases in which MCL-1 is important. As a proof of principle, we generated *huMcl-1; Eμ-Myc* lymphomas and showed that they are more sensitive to
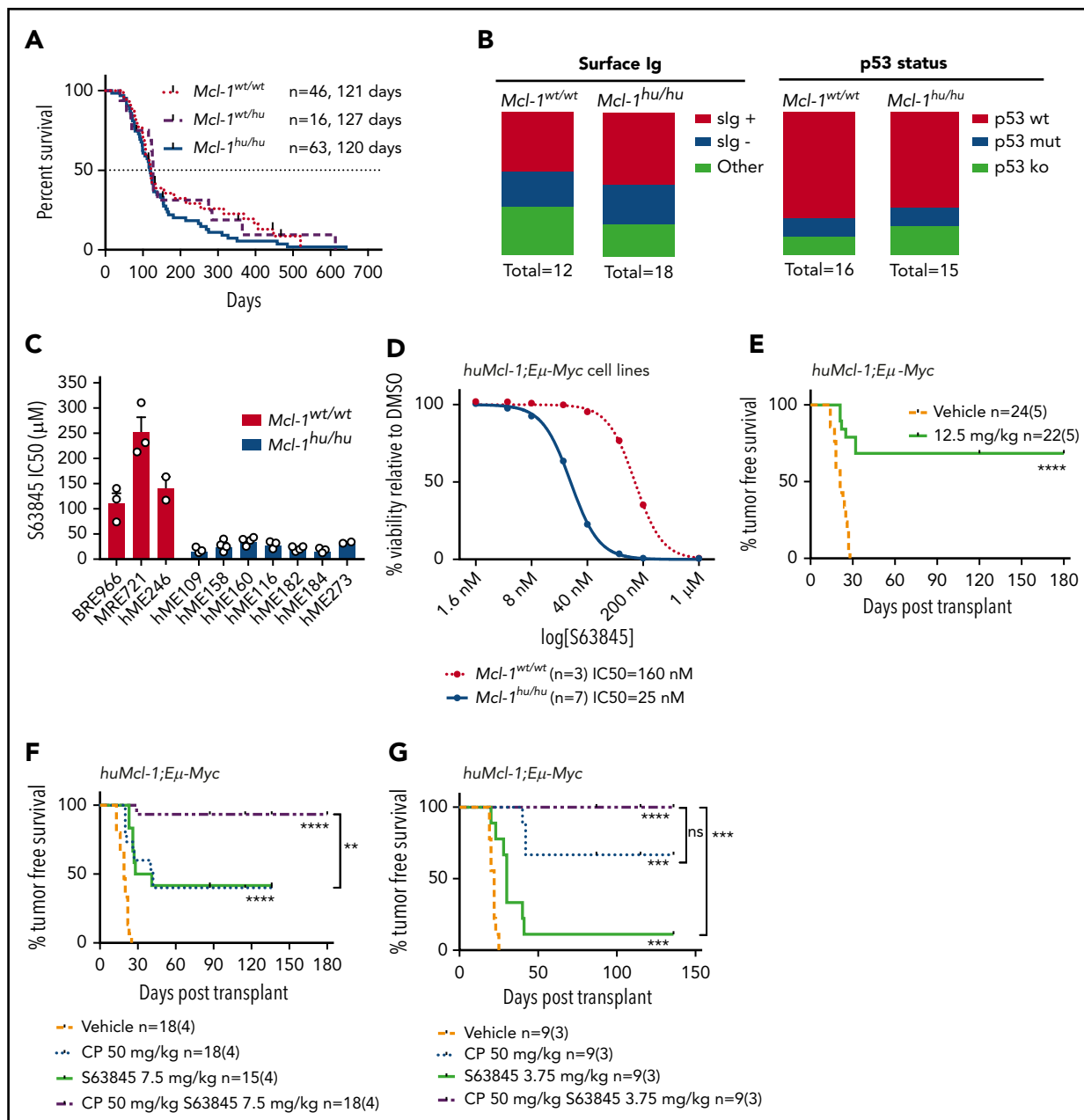
Figure 4. HuMcl-1;Eµ-Myc lymphoma cells are more sensitive to S63845 compared with control Eu-Myc lymphoma cells expressing mouse MCL-1. (A) Eµ-Myc–transgenic mice that were Mcl-1[wt/wt], Mcl-1[wt/hu], or Mcl-1[hu/hu] were aged and monitored for tumor-free survival. Kaplan-Meier survival curve shown with median latency for each genotype. (B) Primary wild-type or huMcl-1 Eµ-Myc lymphoma cells were isolated and immunostained for surface Ig (sIg) expression (IgD and/or IgM) and analyzed by flow cytometry. p53 and p19 expression were detected by western blotting. Proportions of p53 wild-type (p53 low-negative, p19 low-negative), p53 knockout (p53 negative, p19 high), and p53 mutant (p53 high, p19 high) are shown. (C) Viability of Eµ-Myc lymphoma cells that are wild-type for Mcl-1 (n = 3, red bars) or homozygous for the huMcl-1 allele (n = 7, blue bars) after treatment with increasing concentrations of S63845. Cell viability was determined by Annexin V/PI staining and FACS analysis. Data points are IC$_{50}$ values calculated from a range of concentrations (1.6 nM to 1 µM) analyzed in triplicate. (D) Cell viability data generated and shown in panel C were pooled to compare the overall IC$_{50}$ values of control Eµ-Myc and huMcl-1;Eµ-Myc lymphoma cell lines. Combined IC$_{50}$ curves for cell lines of each genotype are shown, with IC$_{50}$ values depicted in the legend. (E-G) Survival curves of huMcl-1;Ly5.1 mice transplanted with huMcl-1;Eµ-Myc lymphomas and treated with vehicle, S63845 alone for 5 consecutive days (E), or S63845 in combination with CP (F-G) (doses as indicated). n indicates the number of recipient mice with number of cell lines tested indicated in parentheses. Significance relative to vehicle shown in graph; significance relative to combination treatment shown on the right. Calculated by Mantel-Cox test. ***P < .001, ****P < .0001. ko, knockout; mut, mutant; ns, not significant; wt, wild-type.

S63845, both in vitro and in vivo, than Eµ-Myc lymphomas expressing mouse MCL-1. The observation that huMcl-1 mice could tolerate doses of S63845 that could prevent growth of huMcl-1;Eµ-Myc lymphomas reinforces the notion that a therapeutic window of MCL-1 inhibitors may be established in the clinic. Although phase 1 clinical trials with MCL-1 inhibitors have

recently commenced, it is important to generate relevant preclinical data in different cancer models using huMcl-1 mice. This will help reach rational decisions on which malignancies will benefit the most and to determine which other anticancer agents can cooperate with MCL-1 inhibitors in tumor cell killing and still be tolerable as a combination therapy.

Acknowledgments

Authorship

Contribution: M.S.B., A.S., G.L.K., and M.J.H. conceived and designed the experiments; M.S.B., C.C., G.D., L.T., and G.L.K. performed experiments; G.L. contributed expertise and provided reagents; and M.S.B., A.S., G.L.K., and M.J.H. wrote the paper with help from the other authors.

Conflict-of-interest disclosure: The authors declare no competing financial interests.

ORCID profiles: M.S.B., 0000-0002-8864-4147; G.L., 0000-0002-1193-8147; A.S., 0000-0002-5020-4891; M.J.H., 0000-0001-7539-7581.

Correspondence: Marco J. Herold, The Walter and Eliza Hall Institute of Medical Research, 1G Royal Parade, Parkville, VIC 3052, Australia; e-mail: herold@wehi.edu.au.

Footnotes

REFERENCES

1. Green DR, Llambi F. Cell death signaling. *Cold Spring Harb Perspect Biol*. 2015;7(12):a006080.

2. Hanahan D, Weinberg RA. Hallmarks of cancer: the next generation. *Cell*. 2011;144(5):646-674.

3. Czabotar PE, Lessene G, Strasser A, Adams JM. Control of apoptosis by the BCL-2 protein family: implications for physiology and therapy. *Nat Rev Mol Cell Biol*. 2014;15(1):49-63.

4. Bhola PD, Letai A. Mitochondria-judges and executioners of cell death sentences. *Mol Cell*. 2016;61(5):695-704.

5. Beroukhim R, Mermel CH, Porter D, et al. The landscape of somatic copy-number alteration across human cancers. *Nature*. 2010;463(7283):899-905.

6. Gong J-N, Khong T, Segal D, et al. Hierarchy for targeting prosurvival BCL2 family proteins in multiple myeloma: pivotal role of MCL1. *Blood*. 2016;128(14):1834-1844.

7. Grabow S, Delbridge AR, Valente LJ, Strasser A. MCL-1 but not BCL-XL is critical for the development and sustained expansion of thymic lymphoma in p53-deficient mice. *Blood*. 2014;124(26):3939-3946.

8. Spinner S, Crispatzu G, Yi JH, et al. Reactivation of mitochondrial apoptosis inhibits T-cell lymphoma survival and treatment resistance. *Leukemia*. 2016;30(7):1520-1530.

9. Kelly GL, Grabow S, Glaser SP, et al. Targeting of MCL-1 kills MYC-driven mouse and human lymphomas even when they bear mutations in p53. *Genes Dev*. 2014;28(1):58-70.

10. Koss B, Morrison J, Perciavalle RM, et al. Requirement for antiapoptotic MCL-1 in the survival of BCR-ABL B-lineage acute lymphoblastic leukemia. *Blood*. 2013;122(9):1587-1598.

11. Glaser SP, Lee EF, Trounson E, et al. Anti-apoptotic Mcl-1 is essential for the development and sustained growth of acute myeloid leukemia. *Genes Dev*. 2012;26(2):120-125.

12. Zhang H, Guttikonda S, Roberts L, et al. Mcl-1 is critical for survival in a subgroup of non-small-cell lung cancer cell lines. *Oncogene*. 2011;30(16):1963-1968.

13. Xiao Y, Nimmer P, Sheppard GS, et al. MCL-1 is a key determinant of breast cancer cell survival: validation of MCL-1 dependency utilizing a highly selective small molecule inhibitor. *Mol Cancer Ther*. 2015;14(8):1837-1847.

14. Roberts AW, Davids MS, Pagel JM, et al. Targeting BCL2 with venetoclax in relapsed chronic lymphocytic leukemia. *N Engl J Med*. 2016;374(4):311-322.

15. Stilgenbauer S, Eichhorst B, Schetelig J, et al. Venetoclax in relapsed or refractory chronic lymphocytic leukaemia with 17p deletion: a multicentre, open-label, phase 2 study. *Lancet Oncol*. 2016;17(6):768-778.

16. Kotschy A, Szlavik Z, Murray J, et al. The MCL1 inhibitor S63845 is tolerable and effective in diverse cancer models. *Nature*. 2016;538(7626):477-482.

17. Weeden CE, Ah-Cann C, Holik AZ, et al. Dual inhibition of BCL-XL and MCL-1 is required to induce tumour regression in lung squamous cell carcinomas sensitive to FGFR inhibition. *Oncogene*. 2018;37(32):4475-4488.

18. Merino D, Whittle JR, Vaillant F, et al. Synergistic action of the MCL-1 inhibitor S63845 with current therapies in preclinical models of triple-negative and HER2-amplified breast cancer. *Sci Transl Med*. 2017;9(401):eaam7049.

19. Kozopas KM, Yang T, Buchan HL, Zhou P, Craig RW. MCL1, a gene expressed in programmed myeloid cell differentiation, has sequence similarity to BCL2. *Proc Natl Acad Sci USA*. 1993;90(8):3516-3520.

20. Rinkenberger JL, Horning S, Klocke B, Roth K, Korsmeyer SJ. Mcl-1 deficiency results in peri-implantation embryonic lethality. *Genes Dev*. 2000;14(1):23-27.

21. Wang X, Bathina M, Lynch J, et al. Deletion of MCL-1 causes lethal cardiac failure and mitochondrial dysfunction. *Genes Dev*. 2013;27(12):1351-1364.

22. Thomas RL, Roberts DJ, Kubli DA, et al. Loss of MCL-1 leads to impaired autophagy and rapid development of heart failure. *Genes Dev*. 2013;27(12):1365-1377.

23. Opferman JT, Iwasaki H, Ong CC, et al. Obligate role of anti-apoptotic MCL-1 in the survival of hematopoietic stem cells. *Science*. 2005;307(5712):1101-1104.

24. Opferman JT, Letai A, Beard C, Sorcinelli MD, Ong CC, Korsmeyer SJ. Development and maintenance of B and T lymphocytes requires antiapoptotic MCL-1. *Nature*. 2003;426(6967):671-676.

25. Vikstrom I, Carotta S, Lüthje K, et al. Mcl-1 is essential for germinal center formation and B cell memory. *Science*. 2010;330(6007):1095-1099.

26. Peperzak V, Vikström I, Walker J, et al. Mcl-1 is essential for the survival of plasma cells. *Nat Immunol*. 2013;14(3):290-297.

27. Dzhagalov I, Dunkle A, He YW. The anti-apoptotic Bcl-2 family member Mcl-1 promotes T lymphocyte survival at multiple stages. *J Immunol*. 2008;181(1):521-528.

28. Huntington ND, Puthalakath H, Gunn P, et al. Interleukin 15-mediated survival of natural killer cells is determined by

interactions among Bim, Noxa and Mcl-1. *Nat Immunol.* 2007;8(8):856-863.

29. Omari S, Waters M, Naranian T, et al. Mcl-1 is a key regulator of the ovarian reserve. *Cell Death Dis.* 2015;6(5):e1755.

30. Dewson G, Kratina T, Sim HW, et al. To trigger apoptosis, Bak exposes its BH3 domain and homodimerizes via BH3:groove interactions. *Mol Cell.* 2008;30(3):369-380.

31. Okamoto T, Coultas L, Metcalf D, et al. Enhanced stability of Mcl1, a prosurvival Bcl2 relative, blunts stress-induced apoptosis, causes male sterility, and promotes

tumorigenesis. *Proc Natl Acad Sci USA.* 2014; 111(1):261-266.

32. Lang MJ, Brennan MS, O'Reilly LA, et al. Characterisation of a novel A1-specific monoclonal antibody. *Cell Death Dis.* 2014; 5(12):e1553.

33. Adams JM, Harris AW, Pinkert CA, et al. The c-myc oncogene driven by immunoglobulin enhancers induces lymphoid malignancy in transgenic mice. *Nature.* 1985;318(6046): 533-538.

34. Ah-Cann C, Tailler M, Kueh AJ, et al. Male sterility in Mcl-1-flox mice is not due to

enhanced Mcl1 protein stability. *Cell Death Dis.* 2016;7(12):e2490.

35. Delbridge AR, Opferman JT, Grabow S, Strasser A. Antagonism between MCL-1 and PUMA governs stem/progenitor cell survival during hematopoietic recovery from stress. *Blood.* 2015;125(21): 3273-3280.

36. Lin X, Morgan-Lappe S, Huang X, et al. 'Seed' analysis of off-target siRNAs reveals an essential role of Mcl-1 in resistance to the small-molecule Bcl-2/Bcl-XL inhibitor ABT-737. *Oncogene.* 2007;26(27): 3972-3979.